Cell Death & Differentiation (2018) 25:885–903
https://doi.org/10.1038/s41418-017-0021-3

Cell Death & Differentiation

ARTICLE

Snail mediates crosstalk between TGFβ and LXRα in hepatocellular carcinoma

Claudia Bellomo[1,2] · Laia Caja[1,2] · Isabel Fabregat[3] · Wolfgang Mikulits[4] · Dimitris Kardassis[5] · Carl-Henrik Heldin[1,2] · Aristidis Moustakas[1,2]

Received: 14 April 2017 / Revised: 17 October 2017 / Accepted: 20 October 2017 / Published online: 11 December 2017

Abstract

Understanding the complexity of changes in differentiation and cell survival in hepatocellular carcinoma (HCC) is essential for the design of new diagnostic tools and therapeutic modalities. In this context, we have analyzed the crosstalk between transforming growth factor β (TGFβ) and liver X receptor α (LXRα) pathways. TGFβ is known to promote cytostatic and pro-apoptotic responses in HCC, and to facilitate mesenchymal differentiation. We here demonstrate that stimulation of the nuclear LXRα receptor system by physiological and clinically useful agonists controls the HCC response to TGFβ. Specifically, LXRα activation antagonizes the mesenchymal, reactive oxygen species and pro-apoptotic responses to TGFβ and the mesenchymal transcription factor Snail mediates this crosstalk. In contrast, LXRα activation and TGFβ cooperate in enforcing cytostasis in HCC, which preserves their epithelial features. LXRα influences Snail expression transcriptionally, acting on the *Snail* promoter. These findings propose that clinically used LXR agonists may find further application to the treatment of aggressive, mesenchymal HCCs, whose progression is chronically dependent on autocrine or paracrine TGFβ.

Introduction

Hepatocellular carcinoma (HCC) is the fifth and seventh cause of cancer worldwide in men and women, respectively, and the third most common cause of cancer death, with leading causative agents being chronic infections by hepatitis B virus and, at a lower degree, hepatitis C virus [1,2]. In HCC, as in other malignancies, transforming growth factor β (TGFβ) has tumor-suppressive and -promoting effects depending on disease stage and microenvironmental context. As tumor suppressor, TGFβ inhibits cell proliferation by inducing transcription of the cell cycle inhibitor genes $p15^{INK4b}$ and $p21^{CIP1}$, and by inducing differentiation, senescence, and apoptosis. TGFβ also hinders mitogen production from stromal cells, impairing inflammatory cytokine secretion from lymphocytes and macrophages [1].

As tumor promoter, TGFβ permits HCC cell proliferation and migration due to desensitization or acquired resistance of hepatocytes to its tumor-suppressive actions [3]. TGFβ induces epithelial–mesenchymal transition (EMT) and anti-apoptotic gene (e.g., *BCL2* and *MCL1*) expression, stimulates synthesis and release of metalloproteinases and pro-fibrotic molecules, thus enhancing invasion and angiogenesis [1]. EMT is driven by the transcription factor Snail

Edited by X. Lu

Electronic supplementary material The online version of this article (https://doi.org/10.1038/s41418-017-0021-3) contains supplementary material, which is available to authorized users.

✉ Aristidis Moustakas
aris.moustakas@imbim.uu.se

1 Department of Medical Biochemistry and Microbiology, Science for Life Laboratory, Box 582, Biomedical Center, Uppsala University, SE-75123 Uppsala, Sweden

2 Ludwig Institute for Cancer Research, Science for Life Laboratory, Box 595, Biomedical Center, Uppsala University, SE-75124 Uppsala, Sweden

3 Bellvitge Biomedical Research Institute (IDIBELL), L'Hospitalet, and Department of Physiological Sciences, School of Medicine, University of Barcelona, ES-08908 Barcelona, Spain

4 Department of Medicine I, Division: Institute of Cancer Research, Comprehensive Cancer Center Vienna, Medical University of Vienna, A-1090 Vienna, Austria

5 Division of Basic Medical Sciences, University of Crete Medical School and Institute of Molecular Biology and Biotechnology, Foundation for Research and Technology of Hellas, GR-71003 Heraklion, Greece

in HCC, which unleashes an invasive phenotype, stem-like functions, and cell survival [2,4].

TGFβ mediates the production of reactive oxygen species (ROS), contributing either to survival or to apoptosis [5]. In rat fetal hepatocytes, ROS induction by TGFβ occurs before the loss of mitochondrial membrane potential, the release of cytochrome C from mitochondria, and the activation of caspase 3, leading to apoptosis [6,7]. Anti-apoptotic ROS are produced by the NADPH oxidase (NOX) 1, and promote epidermal growth factor receptor signaling [5,8]. Under chronic liver cirrhosis, hepatocytes develop resistance to TGFβ-induced apoptosis, a process that is also dependent on ROS, generated by NOX4 [9,10].

Liver X receptors (LXRα/NR1H3 and LXRβ/NR1H2) are transcription factor members of the nuclear hormone receptor family [11]. Oxysterols, derivatives of cholesterol, and its biosynthetic intermediates, such as desmosterols and 24-(S)-25 epoxycholesterol, are physiological ligands and regulate the LXRs [11]. LXRα is expressed in tissues with high metabolic rate, including liver and adipose tissue and macrophages, whereas LXRβ is ubiquitously expressed [11]. LXRs play dual roles in cancer, by suppressing proliferation of cancer cells, or by inhibiting the immunological response via oxysterol production, allowing tumors to escape from immune surveillance [12]. Nonetheless, little evidence exists about the role of LXR and its crosstalk with TGFβ during liver cancer progression.

We recently reported a new mechanism by which LXRα and its agonists counteract TGFβ signaling in fibroblasts, thus blocking their final stage of differentiation into myofibroblasts [13]. Here, we analyzed possible antagonism between TGFβ and LXRα pathways that could affect physiological processes in HCC cells. We report such negative interaction, which, unexpectedly, is mediated by Snail, a regulator of the EMT program.

Results

Oxysterols interfere with TGFβ-induced mesenchymal protein expression in HCC

Based on a high-throughput screen for EMT inhibitors, we established that the LXRα/β agonists T0901317, WYE672, and GW3965 antagonize TGFβ-mediated myofibroblast differentiation, whereas GSK3987, an established LXRα/β antagonist, had neutral or the opposite effect [13]. Along with the oxysterols, ivermectin (a farnesoid-X-receptor agonist) and GGsTOP (a γ-glutamyl-transpeptidase inhibitor) were identified as potential inhibitors of EMT and myofibroblast differentiation [13]. These compounds were tested in combination with TGFβ1 stimulation for 48 h on two HCC models, the epithelial Hep3B and the mesenchymal Snu449 cells [14], in order to assess whether they could revert TGFβ-induced EMT. EMT was analyzed by loss of expression of the epithelial E-cadherin and induction of the mesenchymal proteins fibronectin and vimentin (Fig. 1a). T0901317, WYE672, and GW3965 only slightly decreased the TGFβ-induced expression of fibronectin and essentially failed to restore E-cadherin expression in Hep3B cells (Fig. 1a; for simplicity, each control condition (first lane) shows relative normalized expression set to 1, corresponding to either strong basal expression (E-cadherin) or low basal expression (fibronectin), in order to compare differences in expression between various experimental conditions and the control. The densitometric intensity in the control condition represents the relative abundance of each distinct protein in the respective cell line.). TGFβ signaling potently downregulated E-cadherin and upregulated fibronectin, whereas vimentin, which was already expressed by the mesenchymal Snu449, was further increased (Fig. 1a; for simplicity, the measurable basal levels of E-cadherin, weak basal levels of fibronectin, and appreciable basal levels of vimentin appear as 1 in the quantification of the figure, whereby 1 corresponds to significantly different absolute expression levels. Compare the low levels of E-cadherin ($< 1 \times 10^{-4}$ relative units) after TGFβ1 stimulation and the similarly low levels after use of various compounds in the presence of TGFβ1; or the high levels of fibronectin (21) and vimentin (3) after TGFβ1 stimulation and the similarly high levels after use of most of the compounds in the presence of TGFβ1.). Thus, the LXR agonists could not restore E-cadherin expression in mesenchymal Snu449 cells, but decreased the expression of TGFβ-induced fibronectin and vimentin (Fig. 1a). The results agree with our high-throughput chemical screen [13], and clarify that oxysterols cannot effectively induce mesenchymal to epithelial transition, however, they antagonize TGFβ-dependent regulation of mesenchymal genes.

Impact of TGFβ on LXRα/β expression in HCC cells

We then assessed expression of the *LXRα/β* genes after TGFβ stimulation, using *SERPINE1* as a positive control. In Hep3B cells, *LXRα/NR1H3* expression was unresponsive to TGFβ stimulation and *LXRβ/NR1H2* was upregulated after 16 and 24 h stimulation (Fig. 1b). In Snu449 cells, both *LXRα* and *LXRβ* mRNAs were upregulated (Fig. 1c), LXRα protein expression was enhanced, while LXRβ protein expression remained relatively constant upon TGFβ stimulation (Fig. 1d); inhibitors of p38 (SB203580), JNK (SP600125), and MEK (PD184352) kinases of the MAP-kinase family suppressed the LXRα induction in Snu449 cells, whereas the p38 inhibitor (SB203580) enhanced LXRα levels in the absence of TGFβ stimulation, possibly indicating a stabilizing effect on the LXRα protein (Fig. 1e).

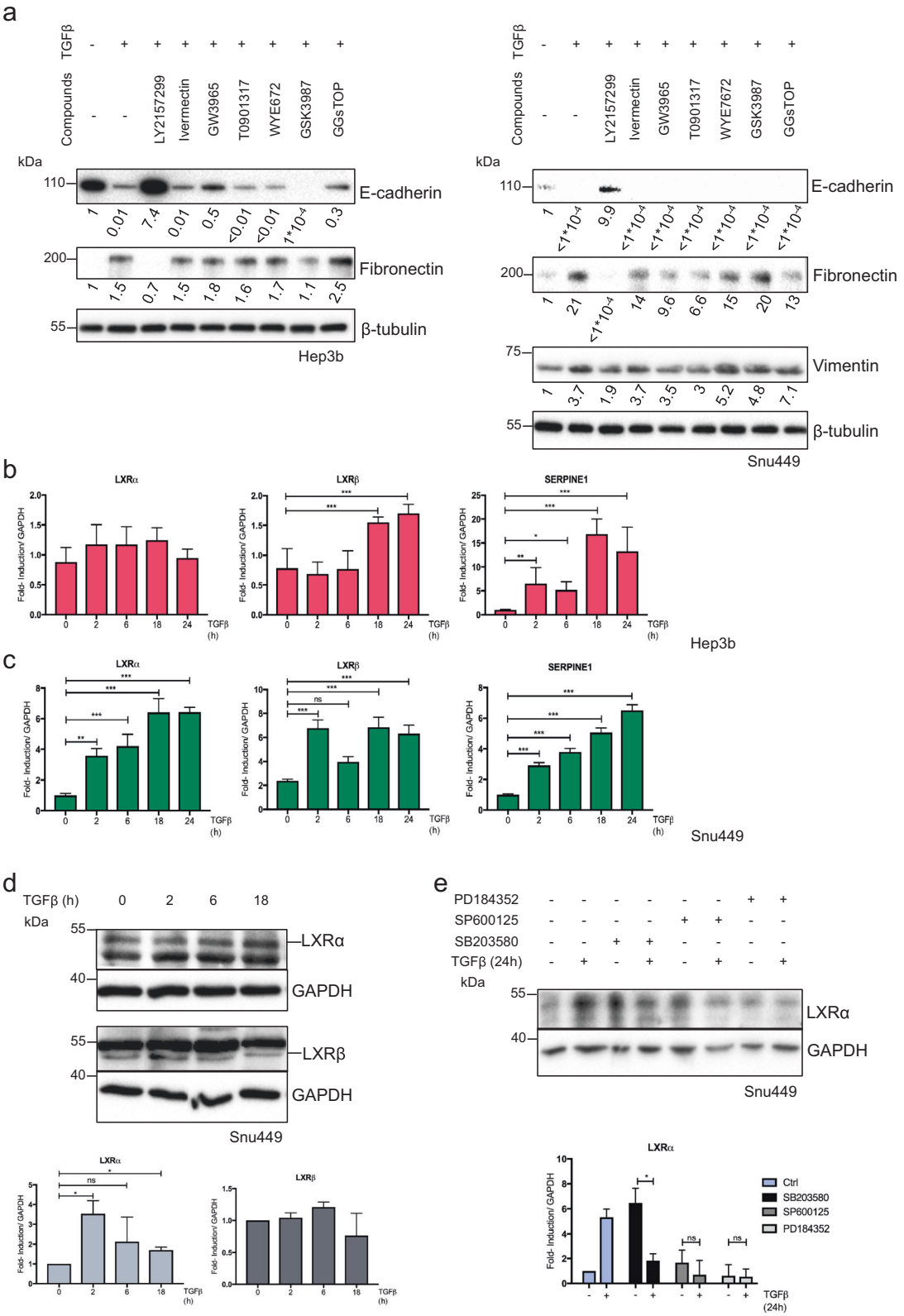

Although the quantification of LXRα/β mRNA and protein levels reports basal level equal to 1 (Fig. 1b–e), this level varies from cell type to cell type and for each LXR member; these differences at the endogenous basal level can be observed in the immunoblots of Fig. 1d, e. In other epithelial HCCs, PLC/PRF5 and HUH7, only *LXRβ* expression was affected by TGFβ stimulation at specific time points, while in mesenchymal HCCs, Snu423, HLE, and HLF,

◀ **Fig. 1 TGFβ regulates LXRα expression in the mesenchymal cell line Snu449. a** Hep3B (left) and Snu449 (right) cells were treated with the indicated compounds (10 μM) and TGFβ1 (5 ng/ml) for 24 h. The TGFβ type I receptor kinase inhibitor LY2157299 was added at a final concentration of 2 μM for 24 h as a potent positive control. The expression of the indicated proteins was analyzed by immunoblotting. Experiments performed in biological duplicate. Densitometric quantification is provided below each lane. Results indicated as <0.01 represent a densitometric intensity between 0.0045 and 0.0082; results indicated as $<1 \times 10^{-4}$ mean a densitometric intensity between 0.00002 and 0.00009; basal expression levels set as 1 correspond to either strong detectable protein levels (E-cadherin) or very low to almost undetectable levels (fibronectin). **b**, **c** Hep3B (**b**) and Snu449 (**c**) cells were treated for different time periods with TGFβ1 (5 ng/ml). The expression of *LXRα*, *LXRβ*, and *SERPINE1*/*PAI1* genes was assessed via real-time PCR and normalized to the expression of *GAPDH*. Mean ± SD values are plotted, and basal expression levels set to 1 correspond to different absolute levels of expression for each mRNA. Experiments performed in biological triplicate, each of them in technical triplicate. **d** Snu449 cells were treated with TGFβ1 (5 ng/ml) for the indicated time periods. The expression of the indicated proteins was analyzed by immunoblotting. Experiments performed in biological triplicate. Densitometric quantification is provided graphically, and basal expression levels set to 1 correspond to different absolute levels of expression for each LXR member. **e** Snu449 cells were treated with vehicle or TGFβ1 (5 ng/ml) for 24 h. SB203580 (p38 inhibitor, 10 μM), SP600125 (JNK inhibitor, 10 μM), and PD184352 (MEK inhibitor, 0.5 μM) were added 1 h prior to TGFβ1 addition. The expression of the indicated proteins was visualized via immunoblotting. Experiments performed in biological triplicate. Densitometric quantification is provided graphically. Statistical significance was assessed by one-way (**b–d**) or two-way (**e**) Anova. Significance was assigned as $*p < 0.05$, $**p < 0.01$, $***p < 0.001$. All immunoblots indicate molecular size markers in kDa

weak level of regulation could be detected for *LXRα* and slightly stronger for *LXRβ* expression after TGFβ treatment (Supplementary Fig. 1). We conclude that TGFβ can regulate LXR levels in certain cell models, but this is not a universal or particularly strong response of HCC to TGFβ.

LXRα activation antagonizes TGFβ-induced Snail expression and nuclear accumulation

The expression of EMT transcription factors and stem cell markers was analyzed in order to assess whether LXRα affected the expression of well-characterized TGFβ target genes (data not shown). Transient LXRα silencing in Snu449 cells caused a significant reduction in the TGFβ-induced expression of *SNAI1* (*Snail*) (Fig. 2a). On the contrary, LXRα overexpression especially in combination with TGFβ stimulation induced Snail mRNA and protein levels (Fig. 2a, b). Activating endogenous LXR with T0901317 suppressed the TGFβ-induced Snail mRNA and protein levels in Snu449 cells (Fig. 2c, d). An independent LXR agonist (GW3965) exhibited the same antagonistic effect (Fig. 2d), suggesting that LXR might interfere with the ability of TGFβ to induce Snail expression in mesenchymal HCC cells. This result was confirmed in additional mesenchymal HCC cells, HLE and HLF, but was not observed in Snu423 cells, or in the epithelial HCC cells PLC/PRF5 and HUH7 (Supplementary Fig. 2).

Stimulating Snu449 cells with TGFβ for 3 h caused a marked nuclear accumulation of Snail protein (Fig. 2e). Co-administration of T0901317 with TGFβ significantly decreased Snail nuclear abundance (Fig. 2e), in agreement with the negative effect on Snail mRNA and protein levels (Fig. 2c, d). Interestingly, the relative distribution of Snail between cytosol and nucleus remained unchanged, but the combined treatment with TGFβ and T0901317 for 24 h decreased Snail protein amounts primarily in the nucleus (Fig. 2f). These observations suggested that the combination treatment might affect Snail transcription rather than its nuclear translocation or stabilization.

LXRα exhibits antagonistic effects over TGFβ on the Snail promoter

To explore transcriptional mechanisms, we employed promoter activation assays in HepG2 cells as a representative HCC cell line that is easy to transfect. In HepG2 cells transfected with the LXR-specific responsive luciferase reporter *ABCA*-luc, stimulation of cells with the two LXR agonists (T0901317 and WYE7672) enhanced reporter activity (Supplementary Fig. S3a); *ABCA*-luc correlated with endogenous *ABCA* and *SREBP1C* gene induction by these agonists in Snu449 cells (Supplementary Fig. S3b). *ABCA* and *SREBP1C* are established gene targets of the LXRs in many cell types. In contrast, the LXR antagonist GSK3987 had a weak negative effect on *ABCA*-luc reporter activity or on endogenous gene expression (Supplementary Fig. 3a, b). To provide specificity of LXR agonist signaling via LXRα, we transiently silenced the endogenous LXRα, causing a lack of response of the *ABCA*-luc reporter or significant reduction in the response of the endogenous genes *ABCA* and *SREBP1C* to the agonist T090137 (Fig. 3a, Supplementary Fig. 3c, d). Monitoring the efficiency of *LXRα* silencing also demonstrated a significant induction of *LXRα* mRNA by the agonist T0901317 (Supplementary Fig. 3c, d). Corroborating these results, LXRα overexpression after transfection of HepG2 cells with the pCMX-LXRα vector [15] activated the *ABCA*-luc promoter and even better after T0901317 stimulation (Fig. 3a). In contrast, a C-terminal deletion mutant of LXRα lacking its ligand-binding domain but retaining DNA-binding and transactivation functions [15], exhibited weak transactivation of the *ABCA*-luc promoter and lack of significant response to T0901317 stimulation (Fig. 3a).

The effect of LXRα silencing and overexpression was determined using an ~900 bp-long human *Snail* promoter fragment cloned upstream of the luciferase reporter [16]. *Snail*-luc activity was readily measurable in the HCC cells;

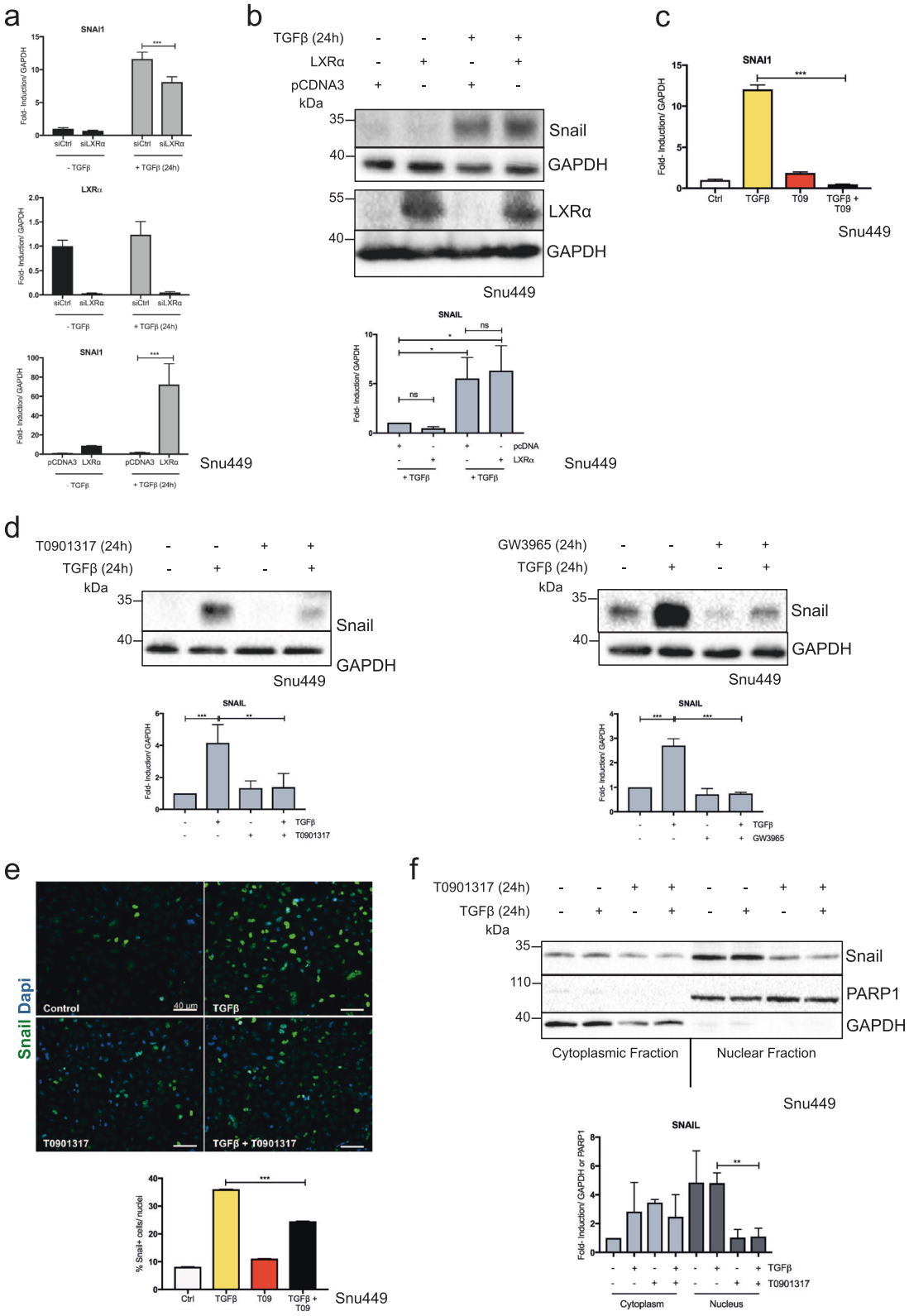

it was significantly abrogated after LXRα silencing and was induced after LXRα overexpression (Fig. 3b). TGFβ stimulation induced *Snail*-luc activity by twofold (Fig. 3c). LXRα overexpression combined with TGFβ stimulation exhibited an even stronger stimulatory effect on the *Snail* promoter (Fig. 3c). However, concomitant stimulation of

◀ **Fig. 2 LXRα activation antagonizes TGFβ-induced Snail expression. a** Snu449 cells were transfected with 30 nM of non-targeting siRNA control or LXRα targeting siRNAs and stimulated by TGFβ1 (5 ng/ml) for 24 h in starvation medium. Expression of the indicated genes was assessed by real-time PCR. Mean ± SD values are plotted, and basal expression levels set to 1 correspond to the same absolute levels of *SNAI1* mRNA expression. Experiments performed in biological duplicate, each of them in technical triplicate. **b** Snu449 were transfected with 1 µg of pCDNA3 or pCMX-LXRα plasmid, and treated with TGFβ1 (5 ng/ml) for 24 h in starvation medium. Expression of the indicated proteins was assessed by immunoblotting. Experiments performed in biological triplicate. Densitometric quantification is provided graphically, and basal expression levels set to 1 correspond to different absolute levels of protein expression, as visualized on the immunoblots. **c** Snu449 cells were treated with TGFβ1 (5 ng/ml) with or without T0901317 (5 µM) in starvation medium for 24 h; expression of *SNAI1* mRNA was assessed by real-time PCR. Mean ± SD values are plotted. Experiments performed in biological triplicate, each of them in technical triplicate. **d** Snu449 cells were treated in starvation medium for 24 h; TGFβ1 (5 ng/ml) was administered with or without LXR agonist (T0901317 or GW3965, 5 µM). Expression of Snail was determined by immunoblotting. Experiments performed in biological quadruplicate. Densitometric quantification is provided graphically, and basal expression level set to 1 corresponds to almost undetectable absolute level of Snail expression, as visualized on the immunoblot. **e** Snu449 cells were immunostained for Snail and DAPI after 3 h of the indicated treatments. Snail is represented in green, DAPI staining in blue. Bars represent 40 µm. Quantification of the percent of Snail-positive nuclei is graphed as mean ± SD values. Experiments performed in biological triplicate. **f** Snu449 cells were starved and treated as specified. Nuclear fractionation assay was performed and abundance of the indicated proteins was assessed by immunoblotting. Experiments performed in biological duplicate. Densitometric quantification is provided graphically, and basal expression levels set to 1 correspond to the cytoplasmic levels of Snail protein expression, as visualized on the immunoblot. Statistical significance was assessed by two-way (**a**, **b**) or one-way (**c–f**) Anova. Significance was assigned as $*p < 0.05$, $**p < 0.01$, $***p < 0.001$. All immunoblots indicate molecular size markers in kDa

the transfected cells with T0901317 resulted in a significant decrease of *Snail*-luc activity (Fig. 3c). This result suggests that only when LXRα is in an active conformation, as enabled by the binding of T0901317 to the LXRα ligand-binding domain, can antagonize the transcriptional effect of TGFβ signaling on Snail. To confirm this finding by an independent assay, we co-expressed Smad3 and Smad4 (mimicking stimulation by exogenous TGFβ), which induced *Snail*-luc activity; when the cells were treated with T0901317 to activate endogenous LXRα, a comparable decrease in *Snail*-luc activity was observed (Fig. 3d). To test the hypothesis that ligand-bound LXRα antagonizes TGFβ signaling on the *Snail* promoter, we repeated the *Snail*-luc experiments using the truncated LXRα mutant that lacks ligand-binding domain. In contrast to full-length LXRα, the truncated mutant failed to enhance *Snail*-luc activity beyond the effect of Smad3/4 and TGFβ, whereas T0901317 lost its ability to suppress the inducibility of *Snail*-luc by TGFβ when administered in the presence of the truncated LXRα mutant (Supplementary Fig. 3e, nonsignificant (ns) difference). During the course of these experiments, we reproducibly observed that whereas T0901317 stabilized LXRα protein levels, TGFβ/Smad signaling destabilized LXRα (Supplementary Fig. 3e, bottom). Taken together, these results suggest that the antagonistic effect between TGFβ and LXRα signaling pathways on Snail occur at the promoter and transcriptional level.

The antagonistic role of LXRα on Snail induction by TGFβ negatively influences the mesenchymal properties of HCC

Combination treatment with TGFβ and T0901317 (Fig. 4a) or GW3965 (Fig. 4b) decreased the Snail-dependent, TGFβ-induced expression of the mesenchymal protein N-cadherin [17]. Co-administration of TGFβ and T0901317 also diminished the localization of N-cadherin at the adherens junctions of the mesenchymal cells, as confirmed by immunocytochemistry (Fig. 4c). EMT is associated with reorganization of the actin cytoskeleton to abundant stress fibers; the combination treatment significantly decreased the formation of actin stress fibers induced by TGFβ stimulation (Fig. 4d). A systematic decrease of mesenchymal features of the Snu449 cells takes place due to the antagonism occurring between the TGFβ and LXR pathways, which correlate with the decrease in Snail expression.

We evaluated whether the described results were dependent on LXRα and consequently on its action on Snail (Fig. 5). The decrease in Snail expression induced by TGFβ and T0901317 co-treatment was rescued after knockdown of LXRα, however the same effect could not be observed for N-cadherin, although a clear trend was recorded (Fig. 5a, statistical analysis). The decrease in N-cadherin localization at adherens junctions and decrease in stress fiber formation by TGFβ and T0901317 co-administration were also rescued when LXRα was silenced (Fig. 5b, c). Thus, the antagonistic effect is dependent on the presence of LXRα, and LXRα activation concomitant to proficient TGFβ causes a decrease in Snail levels, negatively affecting mesenchymal differentiation.

TGFβ and LXRα additively inhibit proliferation of epithelial HCC Hep3B

The epithelial Hep3B cells can undergo cell cycle arrest and apoptosis after TGFβ stimulation, thus resulting in a decrease in cell viability [18]. Co-administration of TGFβ and T0901317 for 48 h in Hep3B cells resulted in even further decreased cell viability when compared to the TGFβ effect alone, as assessed by MTS viability assays (Fig. 6a). The same trend was observed when Hep3B cell proliferation was estimated by Ki67 staining (Fig. 6b). TGFβ treatment caused a decrease in cyclin E and an increase in

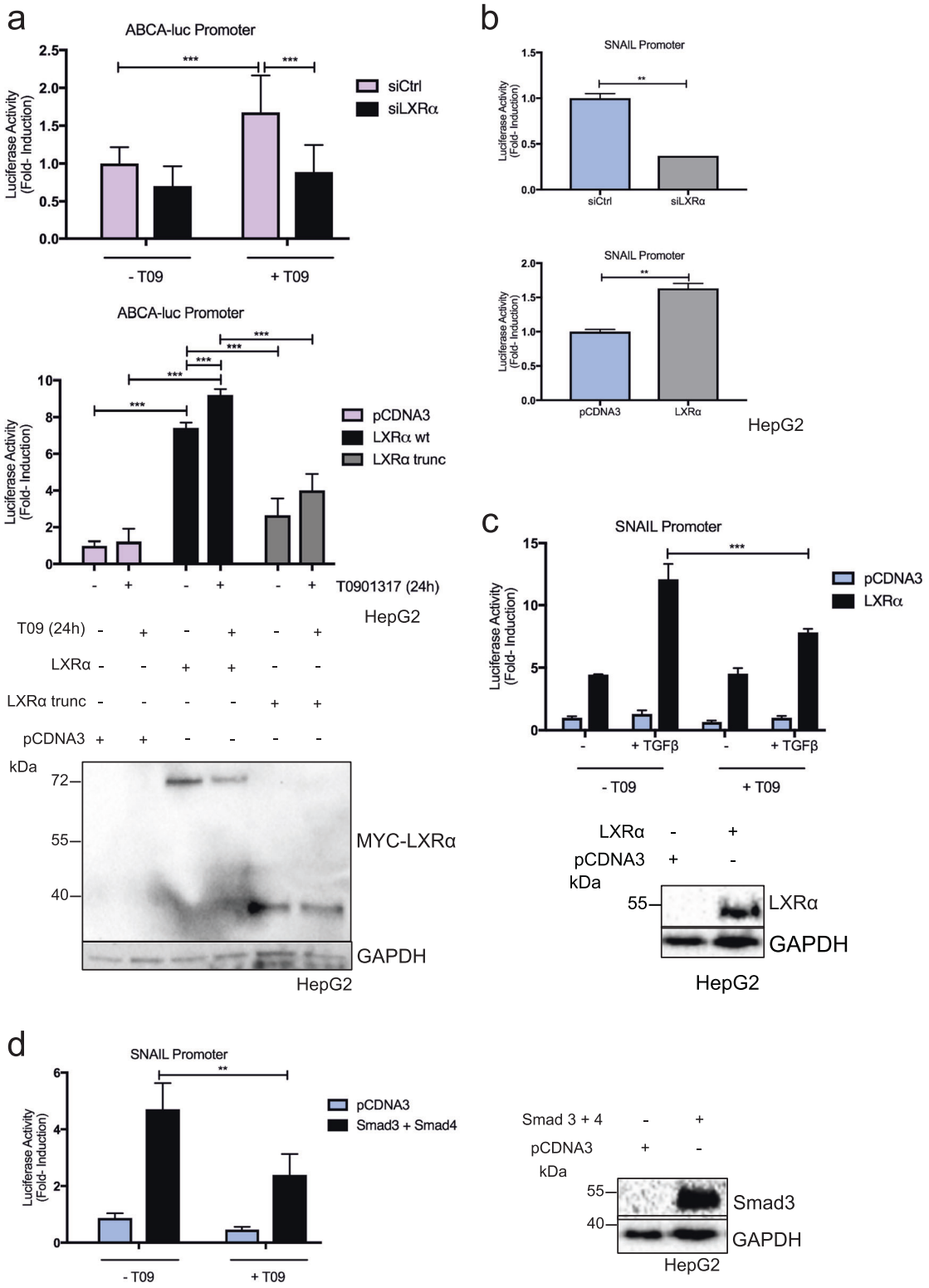

p21^{CIP1} protein expression; these effects were even further enhanced by combination treatment with TGFβ and T0901317 (Fig. 6c), explaining their effects on cell proliferation (Fig. 6a, b). These results define how co-activation of TGFβ and LXRα pathways enhance Hep3B cytostasis, with a strong blockage of Hep3B cells in the G_1 phase, as suggested by strong decrease in Ki67 staining, decrease in cyclin E, and increase in p21^{CIP1} expression.

◀ **Fig. 3 The antagonistic effect of LXRα with regard to TGFβ-induced Snail expression occurs at the promoter level. a** HepG2 cells were simultaneously transfected for 48 h with ABCA1-luc reporter, β-gal plasmid, and siControl non-targeting or siLXRα targeting siRNA at a final concentration of 30 nM (upper graph) or empty vector pCDNA3, pCDNA3-LXRα full length, or pCDNA3-LXRα trunc (bottom graph). Cells were treated in starvation medium with T0901317 (T09, 5 μM) for 24 h, prior to luciferase and β-galactosidase activity detection. Mean ± SD of normalized activity values are plotted, and activity levels set to 1 correspond to the mock (siCtrl or pCDNA3) condition in the presence of DMSO (vehicle), which exhibited different absolute activity levels. Experiments performed in biological triplicate, each of them in technical quadruplicate. Immunoblotting for detection of MYC-tagged LXRα full length or MYC-LXRα trunc together with GAPDH is provided as control. **b** HepG2 cells were simultaneously transfected with **a** siControl non-targeting or siLXRα targeting siRNA at a final concentration of 30 nM and **b** pCDNA3 or pCMX-LXRα and Snail-luciferase reporter plasmids for 48 h prior to luciferase and β-galactosidase activity analysis. Mean ± SD of normalized activity values are plotted, and activity levels set to 1 correspond to the mock (siCtrl or pCDNA3) condition, which exhibited different absolute activity levels. Experiments performed in biological triplicate, each of them in technical triplicate. **c** HepG2 cells were transfected with pCDNA3 or pCMX-LXRα plasmids and Snail-luciferase reporter for 48 h, then treated in starvation medium with TGFβ1 (5 ng/ml) with or without T0901317 (T09, 5 μM) for 24 h, prior to luciferase and β-galactoside activity detection. Mean ± SD of normalized activity values are plotted, and activity levels set to 1 correspond to the mock (pCDNA3) condition in the presence of DMSO (vehicle). Transfected proteins were visualized by immunoblotting. Experiments performed in biological duplicate, each of them in technical quadruplicate. **d** HepG2 cells were transfected with pFlag-Smad3 and -Smad4 and Snail-luciferase reporter plasmids, then cells were treated with T0901317 (T09, 5 μM) for 24 h prior to luciferase and β-galactosidase activity assessment. Mean ± SD of normalized activity values are plotted, and activity levels set to 1 correspond to the mock (pCDNA3) condition in the presence of DMSO (vehicle). Experiments performed in biological triplicate, each of them in technical triplicate. Immunoblotting for detection of Smad3 is provided as control. All immunoblots indicate molecular size markers in kDa. Statistical significance was assessed by two-way (**a**, **c**), one-way (**d**) Anova, or unpaired *T*-test (**b**). Significance was assigned as $^{**}p < 0.01$, $^{***}p < 0.001$

LXRα negatively regulates TGFβ-mediated apoptosis, inducing pro-survival genes

We also asked whether the co-treatment with TGFβ and T0901317 affected the apoptotic pathway in Hep3B cells. Propidium iodide (PI) staining, which marks cells in late apoptosis, suggested that the combination treatment significantly decreased cell death induced by TGFβ (Fig. 7a). Corroborating results were obtained by quantifying caspase 3 cleavage, which is indicative of the early apoptotic response, both in epithelial Hep3B and in mesenchymal Snu449 cells (Fig. 7b). Apoptosis in response to TGFβ also involves antagonism against pro-survival signals of the AKT pathway [2,4]. Accordingly, whereas TGFβ exhibited weak ability to suppress AKT signaling, as measured by phosphorylation of the AKT kinase at Ser473, T0901317 strongly induced AKT phosphorylation, and co-treatment with TGFβ and T0901317 caused an intermediate level in phosphorylated AKT, attesting to the antagonism between these two pathways (Fig. 7c).

In addition to mediating apoptosis, TGFβ can induce the expression of pro-survival and anti-apoptotic proteins, such as BCL-XL, BCL2, MCL1, and XIAP, in conjunction with the acquisition of resistance mechanisms to TGFβ-induced apoptosis [19]. Indeed, the mRNA levels of the pro-survival genes *BCL2* and *MCL1* were increased by TGFβ, and were further enhanced when TGFβ was co-administered with T0901317 in Hep3B cells, suggesting an adaptive mechanism of resistance against apoptosis (Fig. 7d).

Under the same conditions, TGFβ treatment increased ROS production in Hep3B cells by 30%, and this effect was significantly diminished when the LXR pathway was activated together with TGFβ signaling (Fig. 7e). In order to define the molecular determinant of this biological effect, the expression of the enzyme NOX4, previously linked to TGFβ-induced ROS (see introduction), was assessed. TGFβ induced *NOX4* mRNA, while the combination treatment significantly decreased it (Fig. 7f). We conclude that TGFβ and T0901317 cooperate in antagonizing pro-apoptotic responses, by decreasing NOX4 and ROS levels and by enhancing pro-survival gene expression. These results suggest that active LXRα signaling in the presence of TGFβ causes a proliferative blockage with simultaneous resistance to TGFβ-induced apoptosis in HCC cells.

Snail does not influence the apoptotic response but mediates pro-survival gene expression

The decreased Hep3B cell survival observed upon TGFβ and T0901317 co-administration was not regulated by Snail, as assessed by MTS and caspase 3 cleavage assays (Fig. 8a, b) after Snail silencing (Fig. 8f). Snail silencing could slightly but significantly rescue the decrease in ROS production during the combination treatment (Fig. 8c), and the regulation of the *NOX4* gene (Fig. 8d). On the contrary, expression of the pro-survival genes *BCL2* and *MCL1* was dependent on Snail, since silencing Snail significantly abrogated *BCL2* and *MCL1* induction under co-treatment conditions (Fig. 8e). These data suggest that the LXRα agonist counteracts TGFβ signaling leading to apoptosis and requires Snail to induce expression of anti-apoptotic genes and to mediate part of its pro-survival signals, while at the same time, the combinatorial treatment activates other survival pathways. Thus, Snail appears to function as a central regulatory node to fine tune the balance between cell proliferation and apoptosis in HCC.

Discussion

Oxysterols decrease the mesenchymal properties of fibroblasts, suggesting that LXR may antagonize pro-fibrotic

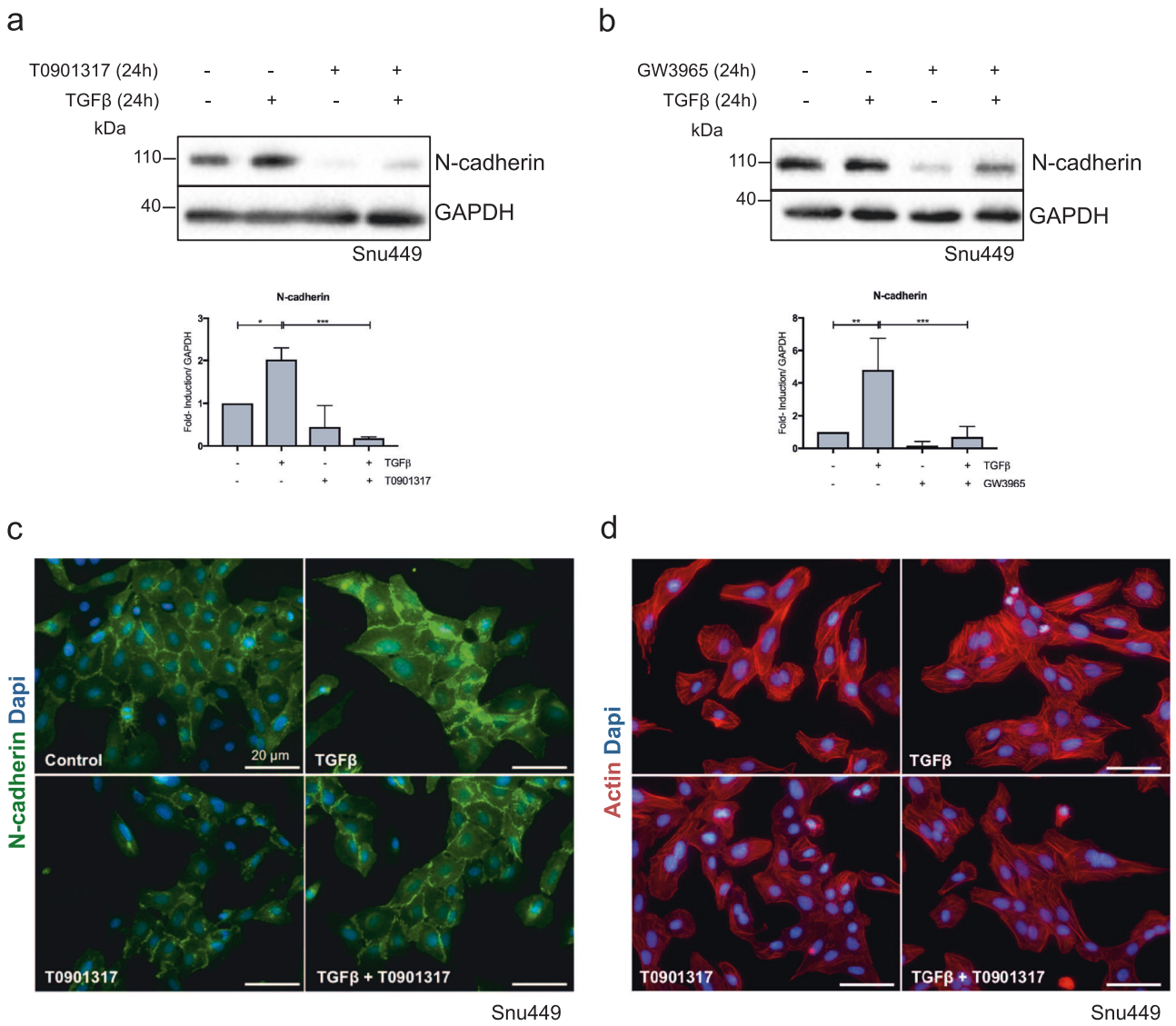

Fig. 4 The antagonistic role of LXRα on TGFβ and Snail negatively influences the mesenchymal properties of Snu449 cells. Snu449 cells were treated with TGFβ1 (5 ng/ml) with or without LXR agonist (T0901317 or GW3965, 5 μM) in starvation medium for 24 h. **a**, **b** The expression of the indicated proteins was assessed by immunoblotting. All immunoblots indicate molecular size markers in kDa. Experiments performed in biological quadruplicate. Densitometric quantification is provided graphically and basal expression levels set to 1 correspond to the different levels of N-cadherin protein expression, as visualized on the immunoblots. Statistical significance was assessed by one-way Anova and was assigned as $*p < 0.05$, $**p < 0.01$, $***p < 0.001$. **c**, **d** Representative images of N-cadherin (green, **c**) immunofluorescence or phalloidin staining shown to visualize F-actin (red, **d**) cellular localization, with DAPI staining in blue. Bars represent 20 μm. Experiments performed in biological triplicate

responses to TGFβ [13]. By focusing on HCC, we identified the transcription factor Snail, as a molecular link of the LXR-TGFβ crosstalk. The new data suggest important actions of LXR during late stages of HCC development, characterized by mesenchymal, aggressive phenotypes.

Analysis of *LXRα* and *LXRβ* gene expression regulation by TGFβ signaling, provided data of relatively weak, time-dependent, and cell type-dependent regulation (Fig. 1, Supplementary Fig. 1). *LXRβ* was regulated by TGFβ signaling more reproducibly (Fig. 1, Supplementary Fig. 1), an observation whose biological significance we have not yet addressed. *LXRα* expression was regulated by MAP-kinase signaling either at basal or TGFβ-induced levels (Fig. 1e). Thus, TGFβ signaling in certain, but not all HCCs, can regulate LXRα/β gene expression.

We examined the link between LXR, TGFβ signaling, and Snail expression, since Snail is an important regulator in both carcinoma cells that undergo EMT and in fibroblasts that respond to TGFβ [20]. In mesenchymal HCC cells, LXRα positively contributed to Snail expression; however, LXRα activation by oxysterols suppressed TGFβ-induced Snail expression (Fig. 2, Supplementary Fig. 2). All

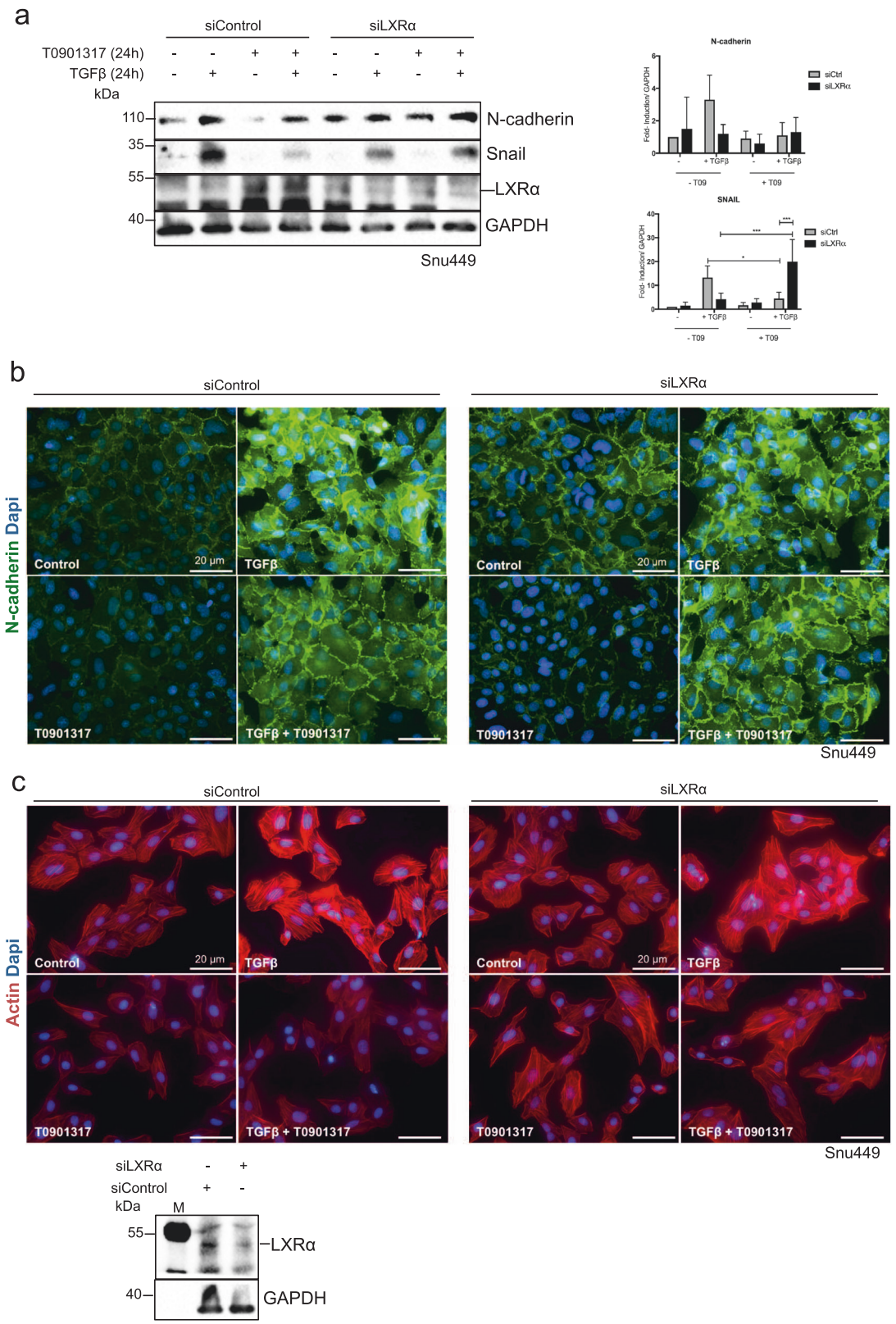

evidence so far supports a model whereby regulation of Snail expression by LXRα is mainly at the transcriptional-promoter level (Figs. 2 and 3). Snail regulates mesenchymal genes and actin fiber organization. LXR agonistic activation suppressed N-cadherin-based junctions and actin stress fibers (Fig. 4), responses supported by endogenous LXRα

◀ **Fig. 5 The antagonistic effect of T0901317 on mesenchymal properties depends on an active LXRα pathway.** Snu449 cells were transfected with non-targeting siControl and siLXRα targeting siRNA for 24 h and treated with TGFβ1 (5 ng/ml) with or without T0901317 (5 μM) in starvation medium for 24 h. **a** The expression of the indicated proteins was assessed by immunoblotting. Experiments performed in biological quadruplicate. Densitometric quantification is provided graphically and basal expression levels set to 1 correspond to different levels of N-cadherin and Snail protein expression, as visualized on the immunoblots. Statistical significance was assessed by two-way Anova and was assigned as $*p < 0.05$, $***p < 0.001$. **b**, **c** Representative images of N-cadherin (green, **b**) immunofluorescence or phalloidin staining to visualize F-actin (red) cellular localization, with DAPI staining in blue. Bars represent 20 μm. Experiments performed in biological triplicate. All immunoblots indicate molecular size markers in kDa; M stands for the molecular size marker lane

(Fig. 5). Previous work in *LXRα*$^{-/-}$ mice established higher Snail expression in epithelial cells surrounding the fibrous bulbs in the ventral prostate [21]. In contrast, in lung adenocarcinoma cells, 25-hydroxycholesterol weakly induced Snail expression via activation of both LXRs [22]. However, these studies did not examine whether these mechanisms involved transcriptional regulation.

Interestingly, LXRα activation by its agonist enhanced the well-established cytostatic effect of TGFβ in epithelial hepatocarcinoma cells [23], by significantly decreasing their viability and proliferation (Fig. 6). The cytostatic effect of TGFβ is based on a block in the G_1 to S phase transition, which was corroborated in this study also based on enhanced induction of the cell cycle inhibitor $p21^{CIP1}$ and decrease in cyclin E levels (Fig. 6). These negative effects of LXRα activation on HCC proliferation agree with previously reported findings of LXRα on cell cycle progression in diverse carcinomas [24–27]. The literature frequently equates cytostasis induced by TGFβ to its pro-apoptotic capacity [2,4]. The evidence provided here clearly distinguishes between these two processes. Whereas LXRα activation enhanced the cytostatic effect of TGFβ, it suppressed pro-apoptotic responses to TGFβ, and even enhanced the expression of pro-survival genes (Fig. 7). Pro-survival molecules such as BCL2, MCL1, and more, can be induced by TGFβ signaling in HCC models, presumably due to a mechanism that aims at counterbalancing pro-apoptotic signals mediated by the same cytokine [4,28,29]. Part of the pro-apoptotic response of HCC to TGFβ is the generation of ROS via the transcriptional induction of NOX4 [30,31]. Even on this front, our study establishes how LXR signaling suppresses the ability of TGFβ to induce NOX4 expression and ROS production (Fig. 7). This provides an additional mechanism by which LXR signaling may counteract pro-apoptotic events in HCC. Thus, LXRα cooperates with TGFβ signaling to generate a strong negative effect on cell proliferation, whereas LXRα antagonizes TGFβ with respect to the apoptotic response. This evidence also suggests that LXRα does not act as a general inhibitor of all TGFβ-mediated physiological actions, but rather, that the two molecular systems interact in maintaining an intermediate state of HCC differentiation and survival, as represented by the apoptosis-resistant, mesenchymal variants of HCC.

While Snail mediated expression of pro-survival *BCL2* and *MCL1* genes (Fig. 8), it was not important for the pro-apoptotic generation of ROS, and only partially affected *NOX4* expression (Fig. 8), in agreement with previous observations [30]. We propose that Snail participates only in a subset of the molecular crosstalk between LXR and TGFβ. Snail mediates TGFβ responses, such as EMT and pro-survival gene expression, whereas the cooperation between LXRα and TGFβ in mediating cytostasis is Snail-independent. LXRα activation in HCC can be beneficial in order to antagonize TGFβ signaling especially in late-stage liver malignancies, via the promotion of a cytostatic, low-mesenchymal HCC status. This could potentially lead to the use of LXR agonists, already in clinical practice, for the treatment of late-stage HCC.

Materials and methods

Cell culture

Hep3B, PLC/PRF5, HUH7, Snu449, Snu423, HLE, and HLF cells have been described before [30,32]. Hep3B cells were cultured in Minimum Essential Medium (Gibco, Thermofisher Scientific, Stockholm, Sweden) supplemented with 10% fetal bovine serum (FBS; Biowest, Almeco A/S, Esbjerg, Denmark) and 100 U/ml penicillin, 100 μg/ml streptomycin, 2 mM glutamine, and 0.1 mM non-essential amino acids (Sigma-Aldrich AB, Stockholm, Sweden). Snu449 and Snu423 were cultured in RPMI-1400 with glutamax (Gibco), 10% FBS and 100 U/ml penicillin, 100 μg/ml streptomycin. PLC/PRF5, HUH7, HLE, HLF, and HepG2 cells were cultured in Dulbecco's modified Eagle medium (Sigma-Aldrich AB) supplemented with 10% FBS and 100 U/ml penicillin, 100 μg/ml streptomycin and 2 mM glutamine (Sigma-Aldrich AB). Cells were kept in a humidified incubator at 37 °C and 5% CO_2.

Screening of compounds

Experiments with inhibitors were performed in 3% FBS-containing medium. TGFβ1 (PeproTech EC Ltd, London, UK), used at a final concentration of 5 ng/ml, was added at the same time as the compounds. Ivermectin, GW3965, GSK3987, WYE672, and GGsTOP (kindly provided by Timothy C. Gahman and Andrew K. Shiau, Ludwig Institute for Cancer Research, La Jolla, CA, USA) were used at a final concentration of 5 or 10 μM, and the TGFβ type I

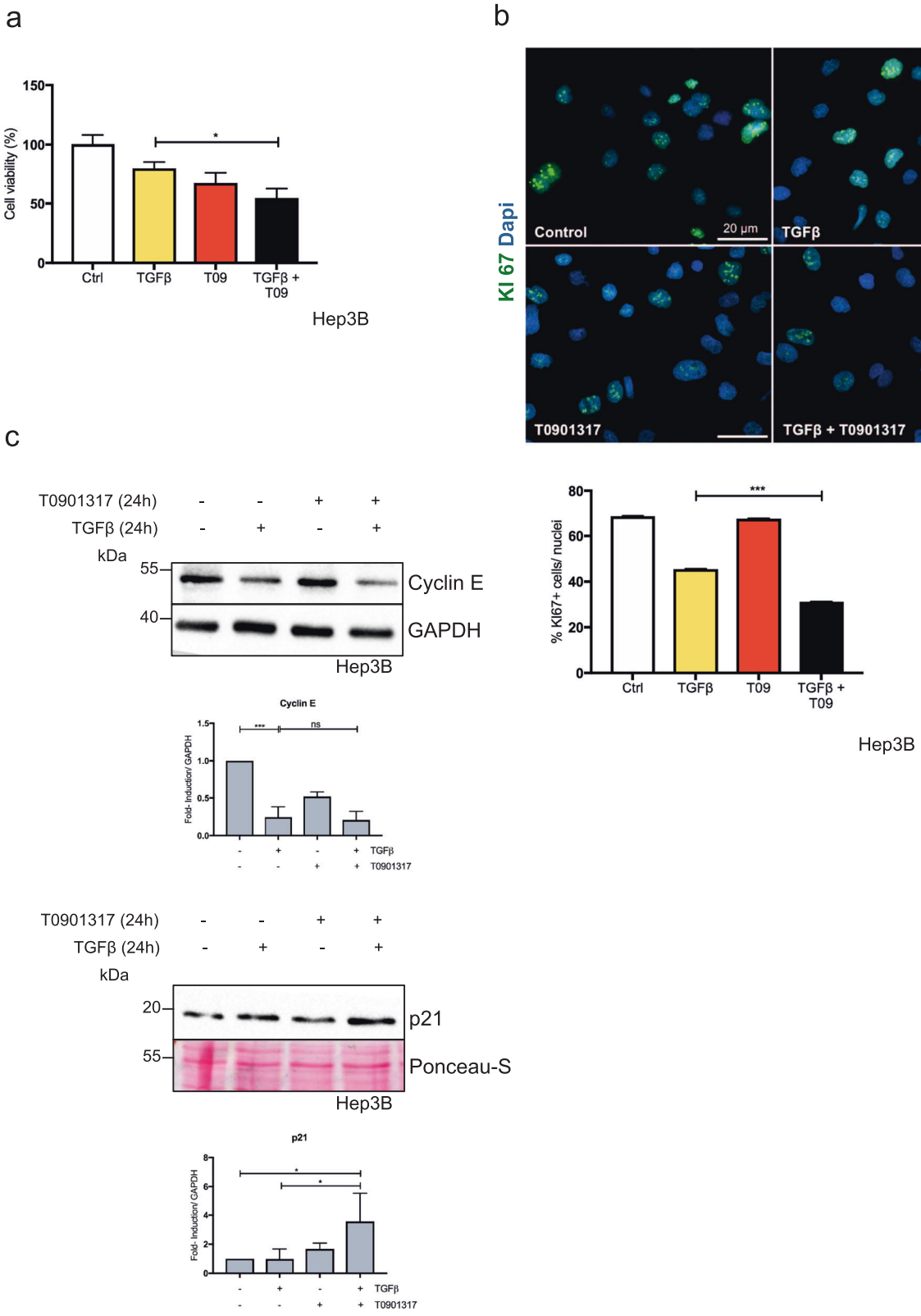

receptor inhibitor LY2157299 (Cayman Chemical, Stockholm, Sweden), at a concentration of 2 μM. Controls were treated with dimethylsulfoxide (Sigma-Aldrich AB), which served as vehicle for dissolving the compounds. Cells were serum-deprived for 16 h, and compounds were added at 80% cell confluency for 48 h. In the case of combination

◀ **Fig. 6 TGFβ and LXRα additively suppress the proliferation of the epithelial Hep3B cells.** Hep3B cells were treated with TGFβ1 (5 ng/ml) with or without T0901317 (5 μM) in starvation medium. **a** Hep3B cells were treated for 48 h and subsequently MTS viability assay was performed. The graph describes the percentage of cell viability related to untreated cells, which is set to 100%, and values are mean ± SD values. Experiments performed in biological triplicate, each of them in technical triplicate. **b** Hep3B cells were treated for 24 h, and immunofluorescence staining for Ki67 was performed. Representative image where Ki67 is represented in green, DAPI staining in blue. Bars represent 20 μm. The percentage of Ki67-positive nuclei is graphed as mean ± SD values, for each condition. Experiments performed in biological triplicate. **c** Hep3B cells were treated for 24 h, the expression of the indicated proteins was assessed by immunoblotting. Experiments performed in biological triplicate. Densitometric quantification is provided graphically and basal expression levels set to 1 correspond to the different absolute levels of cyclin E and p21 protein expression, as visualized on the immunoblots. Statistical significance was assessed by one-way Anova. Significance was assigned as $*p < 0.05$, $***p < 0.001$. All immunoblots indicate molecular size markers in kDa

treatment, TGFβ1 and T0901317 were co-administered to cells at 80% confluency for 24 h. The MAP-kinase inhibitors used were the p38 MAPK inhibitor SB203580 (Calbiochem-Merck, Stockholm, Sweden) at final concentration 10 μM, the JNK inhibitor SP600125 (Calbiochem-Merck) at final concentration 10 μM, and the MEK inhibitor PD184352 (Sigma-Aldrich AB) at final concentration 0.5 μM. Snu449 were seeded at a density of 4×10^5 cells in 60 mm culture dishes, serum-deprived for 16 h prior to treatment with MAP-kinase inhibitors, which were added 1 h prior to treatment with TGFβ1.

SDS-polyacrylamide gel electrophoresis and immunoblotting

For protein extraction, 5×10^5 (Hep3B) and 4×10^5 (Snu449) cells were seeded in 60 mm culture dishes. After the specified treatments, the cells were washed in ice-cold phosphate buffered saline (PBS) pH 7.4 (SVA, Uppsala, Sweden) and lysed in 0.5% Triton X-100, 0.5% sodium deoxycholate, 20 mM Tris-HCl (pH 7.4), 150 mM NaCl, 10 mM EDTA, and 0.25 mM LiCl, supplemented with 25× protease inhibitor cocktail (Roche Diagnostics Scandinavia AB, Bromma, Sweden), 0.25 mM LiCl, 5 mM NaF, and 1 mM Na_3VO_4. Protein concentration was determined by Bradford Assay (Bio-Rad, Hercules, CA, USA). SDS-polyacrylamide gel electrophoresis was performed using 10% or 12% polyacrylamide gels; proteins were transferred to nitrocellulose (0.45 μm) membranes, stained with 0.1% Ponceau-S/5% acetic acid for 5 min at room temperature, and blocked by incubation either in 5% milk or in 5% bovine serum albumin in Tris-buffered saline (0.05 M Tris, 0.138 M NaCl, 0.0027 M KCl, pH 8.0), supplemented with 0.1% Tween 20 (TBS-T), for 1 h at 25 °C. Antibodies against the following proteins were used at the indicated dilutions in TBS-T: fibronectin, 1:10 000 (Sigma-Aldrich AB, F3648); E-cadherin, 1:1000 (BD Biosciences, Stockholm, Sweden, 610182); N-cadherin, 1:1000 (BD Biosciences, 610920); vimentin, 1:2000 (Sigma-Aldrich AB, clone 13:2); claudin 3, 1:1000 (Zymed, Thermofisher Scientific, Stockholm, Sweden, 34-1700); Snail, 1:1000 (Cell Signaling Technology, Stockholm, Sweden, C15D3); PARP1, 1:1000 (BD Pharmingen, Stockholm, Sweden, 556362); PAI1, 1:500 (Abcam, Cambridge, UK, ab66705); pAKT D93 (Ser473), 1:1000 (Cell Signaling Technology, 4060); pan-AKT C67E7, 1:1000 (Cell Signaling Technology, 4691); LXRα, 1:1000 (Abcam, ab41902); LXRβ, 1:1000 (Thermo Scientific Pierce, PA1-333); Cyclin E (M-20), 1:200 (Santa Cruz Biotechnology, Dallas, TX, USA); $p21^{CIP1}$ (EPR362), 1:200 (Abcam, ab109520); GAPDH, 1:50 000 (Ambion, Thermofisher Scientific, Stockholm, Sweden, AM4300); β-tubulin, 1:1000 (BD Pharmingen, 556321); Flag, 1:2000 (Sigma-Aldrich AB); and Myc, 1:5000 (Santa Cruz Biotechnology). Horseradish peroxidase-conjugated anti-mouse, anti-rabbit, or anti-goat secondary antibodies (Invitrogen, Thermofisher Scientific, Stockholm, Sweden) were diluted 1:20 000 in TBS-T solution. Protein bands were visualized by chemiluminescence with the Immobilon Western ECL reagent (Merck-Millipore, Stockholm, Sweden) using the Chemidoc apparatus (Bio-Rad). Densitometric quantification of the bands was performed using Image J software (Image J, NIH). Quantification was performed subtracting the background signal and subsequently normalizing the band representing the protein of interest vs. its loading control (GAPDH or β-tubulin). It is worth noting that normalized expression under basal conditions appears as 1, but this value corresponds to high expression level (e.g., E-cadherin in Fig. 1a, left panel), intermediate to strong expression level (e.g., vimentin in Fig. 1a, right panel), or even very low to almost undetectable expression level (e.g., fibronectin in Fig. 1a, left and right panels).

cDNA synthesis and real-time PCR

For RNA extraction, 5×10^5 (Hep3B) and 4×10^5 (Snu449) cells were seeded in 60 mm culture dishes. Total RNA was isolated using the NucleoSpin RNA II kit (Macherey Nagel, AH Diagnostics, Solna, Sweden) according to the manufacturer's instructions. The extracted RNA was then DNAse I-treated (Life Technologies, Thermofisher Scientific, Stockholm, Sweden) in order to eliminate DNA contaminations, according to the manufacturer's protocol. The extracted RNA was quantified on a NanoDrop 2000 (Thermofisher Scientific, Stockholm, Sweden) and 1 μg was reverse-transcribed to cDNA using the iScript cDNA synthesis kit (Bio-Rad). Real-time PCR was performed based on the primers listed in Supplementary

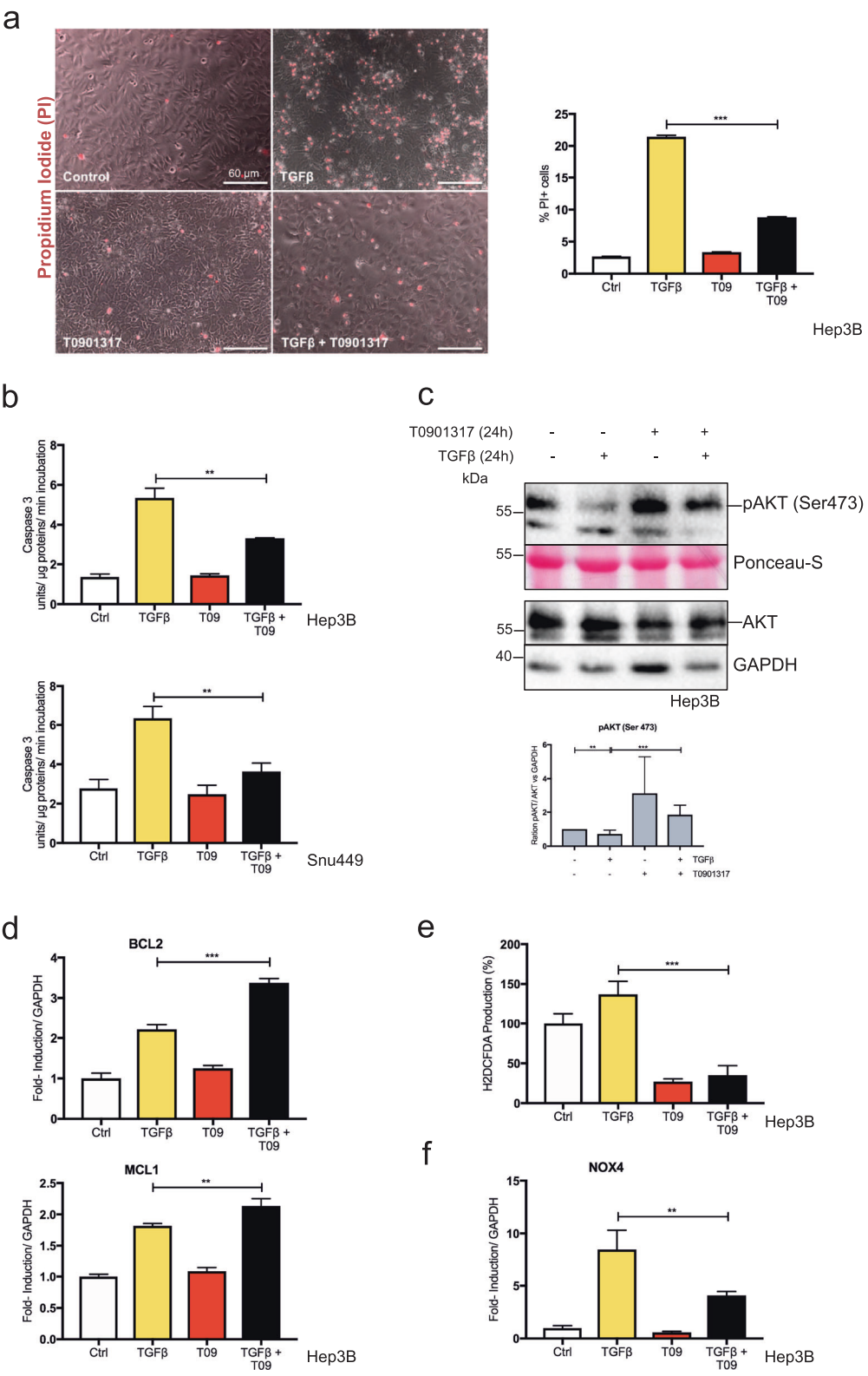

Table 1, on a Bio-Rad CFX96 cycler using KAPA SYBR FAST 2× MasterMix (KAPA, Roche Diagnostics Scandinavia AB) according to the manufacturer's instructions. The expression level of each target gene was normalized to the endogenous reference gene GAPDH and calculated as $2^{-\Delta Ct}$ ($\Delta Ct = Ct_{sample\ mRNA} - Ct_{GAPDH\ mRNA}$). Representative results of at least three biological replicates in technical triplicate are presented.

◀ **Fig. 7 LXRα signaling negatively affects TGFβ induction of early and late apoptosis in Hep3B and Snu449, while inducing pro-survival genes in Hep3B cells.** Cells were treated with TGFβ1 (5 ng/ml) with or without T0901317 (5 μM) in starvation medium. **a** Hep3B cells were treated for 24 h and subsequently stained with propidium iodide (PI), a late apoptosis detection assay. Representative pictures are shown with PI-positive cells (red). Bars represent 60 μm. Quantification of percentage of PI-positive nuclei is graphed as mean ± SD values. Experiments performed in biological triplicate, each of them in technical duplicate. **b** Hep3B cells (left) and Snu449 cells (right) were treated as described in the methods for 16 h and subsequently the caspase 3 cleavage assay was performed, indicative of early apoptosis events. Quantification of caspase activity normalized to protein content per time unit is graphed as mean ± SD values. Experiments performed in biological triplicate, each of them in technical duplicate. **c** Hep3B cells were treated for 24 h, the expression of the indicated proteins was assessed by immunoblotting. Experiments performed in biological triplicate. Densitometric quantification is provided graphically, and basal expression levels set to 1 correspond to the levels of pAKT protein in the presence of vehicle treatment, as visualized on the immunoblot. All immunoblots indicate molecular size markers in kDa. **d** Hep3B cells were treated in starvation medium for 16 h, as described in the methods. The expression of the indicated genes was assessed via real-time PCR and is graphed as mean ± SD values, and basal expression levels set to 1 correspond to different absolute levels of *BCL2* or *MCL1* mRNA expression. Experiments performed in biological triplicate, each of them in technical triplicate. **e** After 4 h of treatment, the total amount of reactive oxygen species was quantified by H2DCFDA fluorimetric quantification. Data are presented as percentage vs. control, which is set to 100%, and are mean ± SD. Experiments performed in biological quadruplicate, each of them in technical duplicate. **f** Upon 16 h treatment, the expression of *NOX4* mRNA was assessed via real-time PCR, and results are shown as mean ± SD. Experiments performed in biological triplicate, each of them in technical triplicate. Statistical significance was assessed by one-way Anova. Significance assigned $^{**}p < 0.01$, $^{***}p < 0.001$

Transient transfection with siRNA

Hep3B and Snu449 cells were seeded at a density of 1×10^6 in 15 cm culture dishes and transiently transfected with the indicated siRNA. Cells were transfected at ~80% confluency in serum-free OptiMem (Gibco, Thermofisher Scientific), and Mirus TransIT siQUEST (Mirus Biological, Kem En Tech Diagnostics Nordics, Taastrup, Denmark) as transfection reagent, according to the manufacturer's guidelines. After 24 h cells were seeded for subsequent experiments at specified densities, as described. Where specified, cells where serum-starved for 16 h and subsequently TGFβ1-treated with or without T0901317 for the indicated time periods at 5 ng/ml and 5 μM, respectively. The used siRNAs were as follows: siControl (ON-TARGETplus Non-targeting Pool #D-001810-10-20, Dharmacon); siLXRα (ON-TARGETplus Human NR1H3 siRNA SMARTpool L-003413-00-0005, Dharmacon); and siSNAI1 (ON-TARGETplus Human SNAI1 siRNA SMARTpool L-010847-01-0005, Dharmacon).

Transient overexpression

Hep3B cells were seeded at a density of 5×10^5 cells in 60 mm culture dishes and transient overexpression was performed with the indicated plasmids (final total DNA of 1 μg). Cells were transfected at ~80% confluency using OptiMem (Gibco, Thermofisher Scientific) and Mirus TransITX2 (Mirus Biological, Kem En Tech Diagnostics Nordics) as transfection reagent, according to the manufacturer's guidelines. Transfection was performed for 24 h and, where indicated, cells were subsequently serum-starved for 16 h and then TGFβ1-treated (5 ng/ml) with or without T0901317 (5 μM) for the indicated time periods. The plasmids used were pCDNA3 as mock control, pABCA1-luc, pCMX-LXRα, and pCMX-LXRα trunc, the latter three as previously described [15], and pCMV-β-galactosidase, phSnail-promoter-luc, pCDNA3-Flag-Smad3, and pCDNA3-Flag-Smad4, as described [33].

Cytoplasmic-nuclear fractionation

Snu449 cells were seeded at a density of 4×10^5 cells in 60 mm culture dishes. Cells were serum-deprived for 16 h prior to treatments with TGFβ1 (5 ng/ml) and/or T0901317 (5 μM). In the case of combination treatment, TGFβ1 and T0901317 were co-administered for 3 h. Treatments were performed at 80% cell confluency. Nuclear fractionation was performed using the CelLytic NuCLEAR Extraction Kit (Sigma-Aldrich AB) according to the manufacturer's instructions. Proteins were identified via immunoblotting, as described above.

Immunocytochemistry

Snu449 cells were seeded at a density of 3×10^5 cells on glass coverslips in six-well dishes, serum-deprived for 16 h prior to treatments with TGFβ1 (5 ng/ml) and/or T0901317 (5 μM). Treatments were performed at 80% confluency for N-cadherin and Snail staining and 60% confluency for Ki67 and phalloidin-actin staining. Cells were washed twice with PBS and subsequently fixed in 4% formaldehyde/PBS for 30 min (Ki67, phalloidin-actin, and Snail stainings) or fixed in ice-cold methanol:acetone for 10 min (N-cadherin staining). Cells were washed three times with PBS, permeabilized with freshly made 0.5% Triton X-100/PBS for 10 min, subsequently washed three times with PBS, and blocked with 5% FBS/PBS–0.1 M glycine for 16 h at 4 °C. Slides were washed three times with PBS and subsequently incubated with primary antibodies in 5% FBS/PBS–0.1 M glycine for 3 h or phalloidin for 30 min at room temperature (25 °C). The fixed cells were incubated with the appropriate Alexa Fluor-488 secondary antibody (Invitrogen, Thermofisher Scientific) at a dilution of 1:1000 in PBS for 1 h in the

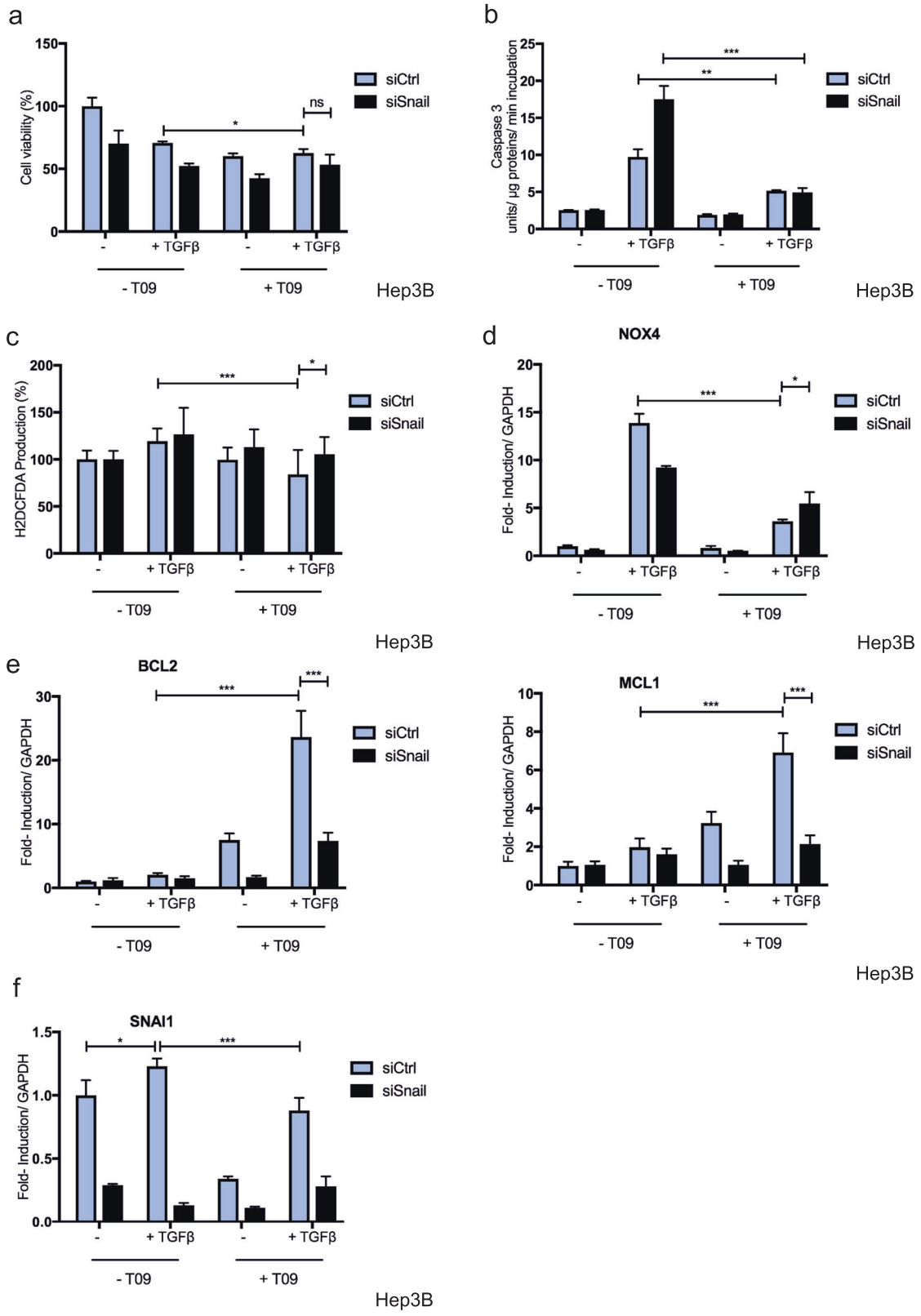

dark, at room temperature. Finally, incubation with 4′,6-diamidino-2-phenylindole (Sigma-Aldrich AB) at a dilution of 1:1000 in PBS was performed for 5 min. Coverslips were mounted on microscope slides with Fluoromount G (SouthernBiotech, AH Diagnostics, Solna, Sweden) and observed on a Nikon Eclipse 90i fluorescence microscope.

◀ **Fig. 8 Snail regulates the expression of pro-survival genes *BCL2* and *MCL1*.** Hep3B cells were transfected with non-targeting siControl and siSnail targeting siRNA at a final concentration of 30 nM for 24 h and subsequently seeded for the specified experiments, then cells were treated with TGFβ1 (5 ng/ml) with or without T0901317 (5 μM) in starvation medium. **a** Cells were treated for 48 h and the cell viability was assessed by MTS assay. The graph reports the percentage of cell viability related to untreated cells transfected with siCtrl, which is set to 100%, as mean ± SD values. Experiments performed in biological triplicate, each of them in technical triplicate. **b** Hep3B cells were treated for 16 h, then caspase 3 cleavage assay was performed; quantification of caspase activity normalized to protein content per time unit is graphed as mean ± SD values. Experiments performed in biological triplicate, each of them in technical duplicate. **c** After 4 h of treatment, H2DCFDA fluorimetric quantification was performed. Data are presented as percentage vs. control, which is set to 100%, and are mean ± SD. Experiments performed in biological quadruplicate, each of them in technical duplicate. **d–f** Hep3B cells were incubated with or without T0901317 for 16 h; the expression of genes of interest was then analyzed by real-time PCR and the results are described as mean ± SD, with basal expression levels set to 1, corresponding to different absolute levels of *BCL2*, *MCL1*, or *SNAI1* mRNA expression. Experiments performed in biological triplicate, each of them in technical triplicate. Statistical significance was assessed by one-way (**b**) or two-way (**a**, **c**-**f**) Anova. Significance was assigned as $*p < 0.05$, $**p < 0.01$, $***p < 0.001$

Primary images were acquired using the NIS elements software. The primary reagents used for staining were antibodies against Snail (1:200 dilution; Cell Signaling Technology, C15D3), N-cadherin (1:200 dilution; BD Biosciences, 610920), Ki67 (1:200 dilution; Abcam, ab15580), and TRITC-conjugated phalloidin (1:1000 dilution; Sigma-Aldrich AB).

Luciferase assay

HepG2 cells were seeded at a density of 18×10^3 cells in 24-well dishes. Cells were transfected with a human *SNAIL* promoter construct encompassing approximately 900 bp fused to the luciferase cDNA [33] or the proximal promoter of the LXRα target gene *ATP binding cassette transporter A1* (*ABCA1*) fused to luciferase, together with pCMV-β-galactosidase plasmid, the latter used as reference control, at final amount of 100 ng per plasmid DNA. Transient overexpression was performed with the indicated plasmids, while transient silencing was conducted with the indicated siRNAs at a final concentration of 30 nM. Transfection was performed when cells were ~80% confluent for 48 h, as explained above. Where indicated, cells were subsequently serum-starved for 16 h and then TGFβ1 (5 ng/ml) or T0901317 (5 μM), or a combination thereof were added for the indicated time periods. Luciferase assay was performed using the Firefly Luciferase Assay Kit (Biotium, Techtum, Stockholm, Sweden) according to the manufacturer's instructions. β-Galactosidase activity was assessed via quantification of conversion of its substrate o-nitrophenol-glucose at 420 nm, and used as control. Chemiluminescent and colorimetric readings were performed in an Enspire Multimode multiwell 96-plate reader (Perkin Elmer, Upplands Väsby, Sweden).

Cell viability (MTS) assay

Hep3B cells were seeded at a density of 8×10^3 cells in 96-well dishes, serum-starved for 16 h, and then, when they had reached 80% confluency, were incubated with TGFβ1 (5 ng/ml) or T0901317 (5 μM), or a combination thereof for 48 h. Where indicated, Hep3B cells were seeded at a density of 1×10^6 cells in 15 cm dishes and transiently transfected with the indicated siRNAs at a final concentration of 30 nM for 24 h, as described above. Afterwards, cells were seeded at the indicated concentration, serum-starved, and treated as reported. MTS assay was performed using the CellTiter 96 AQueous One Solution Cell Proliferation Assay kit (Promega, Stockholm, Sweden) according to the manufacturer's instructions. The MTS solution was diluted in a 1:10 ratio with cell media and the incubation was performed in dark for 2 h in a humidified incubator at 37 °C, 5% CO_2. The absorbance of formazan salts was read at 490 nm in an Enspire Multimode multiwell 96-plate reader (Perkin Elmer). Representative results of at least three biological replicates in technical triplicate are presented.

Caspase 3 activity assay (early apoptosis)

Hep3B cells were seeded at a density of 5×10^5 cells in 60 mm dishes, serum-starved for 16 h, and then, when they had reached 80% confluency, cells were incubated with TGFβ1 (5 ng/ml) or T0901317 (5 μM), or a combination thereof for 16 h. Where indicated, Hep3B cells were transiently transfected with the indicated siRNAs, as previously described. Afterwards, cells were seeded at the indicated concentration, serum-starved, and treated as reported. After treatment, cell media was collected and cells were scraped in 3 ml PBS (pH 7.4); cell media and lysates were centrifuged at 2500 r.p.m. for 10 min at 4 °C. The pellet was then resuspended in a solution containing 5 mM Tris-HCl pH 8, 20 mM EDTA, 0.5% Triton X-100, vortexed for 10 s, incubated on ice for 10 min, and centrifuged at 13 000 r.p.m. for 10 min at 4 °C. Protein quantification was performed via Bradford Assay (Bio-Rad). Proteins (25 μg) were resuspended in reaction buffer, containing 1 M HEPES (pH 7.5), 87% glycerol, 1 M dithiothreitol, and the Ac-DEVD-AMC Caspase 3 fluorogenic substrate (BD Biosciences) was added at a concentration established by the manufacturer. Incubation was then performed in dark for 2 h in a humidified incubator at 37 °C, 5% CO_2. Fluorimetric analysis was performed in an Enspire Multimode multiwell 96-plate reader (Perkin Elmer). Fluorimetric caspase 3 activity was normalized vs.

the time of incubation of the substrate and the protein content. Representative results of at least three biological replicates in technical duplicate are presented.

PI assay (late apoptosis)

Hep3B cells were seeded at a density of 3×10^5 cells in six-well dishes, serum-starved for 16 h, and then, at 80% confluency, cells were treated with TGFβ1 (5 ng/ml) or T0901317 (5 μM), or a combination thereof for 24 h. PI solution was then diluted in a 1:200 ratio with cell media and the incubation was performed in the dark for 10 min in a humidified incubator at 37 °C, 5% CO_2. Incubation of PI was performed serially for each condition and was immediately followed by microscopic evaluation of each single condition, in order to avoid excessive permeation of PI into cells over prolonged time. Phase contrast images were observed with a ×10 objective in a Zeiss Axioplan microscope using a Zeiss Axioplan MRC digital camera. Primary images were acquired and adjusted using the Zen 2011 software.

2´´,7´-Dichlorodihydrofluorescein diacetate assay (oxidative stress)

Hep3B cells were seeded at a density of 4×10^4 cells in 12-well dishes, serum-starved for 16 h, and then, at 80% confluency, cells were treated with TGFβ1 (5 ng/ml) or T0901317 (5 μM), or a combination thereof for 16 h. Where indicated, Hep3B cells were transiently transfected with the indicated siRNAs, as described above. Afterwards, cells were seeded at the indicated concentration, serum-starved, and treated as described. After treatment, cells were incubated with 2.5 μM 2″,7′-dichlorodihydrofluorescein diacetate (Invitrogen, Thermofisher Scientific) in HBSS without red phenol for 30 min. Cells were subsequently lysed with a buffer containing 25 mM HEPES (pH 7.5), 60 mM NaCl, 1.5 mM $MgCl_2$, 0.2 mM EDTA, and 0.1% Triton X-100 for 10 min at 4 °C. Fluorescence analysis was performed in an Enspire Multimode 96-well plate reader (Perkin Elmer). Fluorescence values were normalized relative to the protein content and are presented as percentage of control. Average of four independent biological replicates in technical duplicate is presented.

Statistical analysis

Experiments were performed in biological replicates, each of which included at minimum technical triplicates, as indicated in the figure legends. Representative results are reported as averages minus-plus SD. Statistical analysis was performed with GraphPadPrism (La Jolla, CA, USA) using the specific analytical formula explained in the figure legend, and statistical significance * was assigned with p value < 0.05, $^{**}p < 0.01$, $^{***}p < 0.001$.

Acknowledgements This work was supported by the Ludwig Institute for Cancer Research, the Swedish Cancer Society (project numbers: CAN 2012/438 and CAN 2015/438 to A.M.; CAN 2016/445 to C.-H. H.; and CAN 2012/1186 to L.C.), the Swedish Research Council (project numbers K2013-66X-14936-10-5 to A.M. and 2015-02757 to C.-H.H.), and the EU FP7 ITN IT-LIVER (to A.M.). We thank Timothy C. Gahman and Andrew K. Shiau, Ludwig Institute for Cancer Research, La Jolla, CA, USA, for LXR agonist/antagonist synthesis. We also thank members of our group and all members of the IT-Liver (www.it-liver.eu) for suggestions and useful discussions.

Compliance with ethical standards

Conflict of interest The authors declare that they have no conflict of interests.

References

1. Majumdar A, Curley SA, Wu X, Brown P, Hwang JP, Shetty K, et al Hepatic stem cells and transforming growth factor β in hepatocellular carcinoma. Nat Rev Gastroenterol Hepatol. 2012;9:530–8.
2. Dooley S, ten Dijke P. TGF-β in progression of liver disease. Cell Tissue Res. 2012;347:245–56.
3. Meindl-Beinker NM, Matsuzaki K, Dooley S. TGF-β signaling in onset and progression of hepatocellular carcinoma. Dig Dis. 2012;30:514–23.
4. Fabregat I. Dysregulation of apoptosis in hepatocellular carcinoma cells. World J Gastroenterol. 2009;15:513–20.
5. Murillo MM, Carmona-Cuenca I, Del Castillo G, Ortiz C, Roncero C, Sanchez A, et al Activation of NADPH oxidase by transforming growth factor-β in hepatocytes mediates up-regulation of epidermal growth factor receptor ligands through a nuclear factor-κB-dependent mechanism. Biochem J. 2007;405:251–9.
6. Herrera B, Alvarez AM, Sanchez A, Fernandez M, Roncero C, Benito M, et al Reactive oxygen species (ROS) mediates the mitochondrial-dependent apoptosis induced by transforming growth factor β in fetal hepatocytes. FASEB J. 2001;15:741–51.
7. Herrera B, Fernandez M, Alvarez AM, Roncero C, Benito M, Gil J, *et al* Activation of caspases occurs downstream from radical oxygen species production, Bcl-xL down-regulation, and early cytochrome C release in apoptosis induced by transforming growth factor β in rat fetal hepatocytes. Hepatology. 2001;34:548–56.

8. Sancho P, Bertran E, Caja L, Carmona-Cuenca I, Murillo MM, Fabregat I. The inhibition of the epidermal growth factor (EGF) pathway enhances TGF-β-induced apoptosis in rat hepatoma cells through inducing oxidative stress coincident with a change in the expression pattern of the NADPH oxidases (NOX) isoforms. Biochim Biophys Acta. 2009;1793:253–63.
9. Shima Y, Nakao K, Nakashima T, Kawakami A, Nakata K, Hamasaki K, et al Activation of caspase-8 in transforming growth factor-β-induced apoptosis of human hepatoma cells. Hepatology. 1999;30:1215–22.
10. Black D, Bird MA, Samson CM, Lyman S, Lange PA, Schrum LW, et al Primary cirrhotic hepatocytes resist TGFβ-induced apoptosis through a ROS-dependent mechanism. J Hepatol. 2004;40:942–51.
11. Calkin AC, Tontonoz P. Transcriptional integration of metabolism by the nuclear sterol-activated receptors LXR and FXR. Nat Rev Mol Cell Biol. 2012;13:213–24.
12. Jakobsson T, Treuter E, Gustafsson JA, Steffensen KR. Liver X receptor biology and pharmacology: new pathways, challenges and opportunities. Trends Pharmacol Sci. 2012;33:394–404.
13. Carthy JM, Stöter M, Bellomo C, Vanlandewijck M, Heldin A, Morén A, et al Chemical regulators of epithelial plasticity reveal a nuclear receptor pathway controlling myofibroblast differentiation. Sci Rep. 2016;6:29868.
14. Coulouarn C, Factor VM, Thorgeirsson SS. Transforming growth factor-β gene expression signature in mouse hepatocytes predicts clinical outcome in human cancer. Hepatology. 2008;47:2059–67.
15. Thymiakou E, Zannis VI, Kardassis D. Physical and functional interactions between liver X receptor/retinoid X receptor and Sp1 modulate the transcriptional induction of the human ATP binding cassette transporter A1 gene by oxysterols and retinoids. Biochemistry. 2007;46:11473–83.
16. Tan E-J, Thuault S, Caja L, Carletti T, Heldin C-H, Moustakas A. Regulation of transcription factor Twist expression by the DNA architectural protein high mobility group A2 during epithelial-to-mesenchymal transition. J Biol Chem. 2012;287:7134–45.
17. Oda H, Tsukita S, Takeichi M. Dynamic behavior of the cadherin-based cell-cell adhesion system during Drosophila gastrulation. Dev Biol. 1998;203:435–50.
18. Caja L, Sancho P, Bertran E, Fabregat I. Dissecting the effect of targeting the epidermal growth factor receptor on TGF-β-induced-apoptosis in human hepatocellular carcinoma cells. J Hepatol. 2011;55:351–8.
19. Fabregat I, Roncero C, Fernandez M. Survival and apoptosis: a dysregulated balance in liver cancer. Liver Int. 2007;27:155–62.
20. Bellomo C, Caja L, Moustakas A. Transforming growth factor β as regulator of cancer stemness and metastasis. Br J Cancer. 2016;115:761–9.
21. Kim HJ, Andersson LC, Bouton D, Warner M, Gustafsson J-A. Stromal growth and epithelial cell proliferation in ventral prostates of liver X receptor knockout mice. Proc Natl Acad Sci USA. 2009;106:558–63.
22. Chen L, Zhang L, Xian G, Lv Y, Lin Y, Wang Y. 25-Hydroxycholesterol promotes migration and invasion of lung adenocarcinoma cells. Biochem Biophys Res Commun. 2017;484:857–63.
23. Inagaki M, Moustakas A, Lin H-Y, Lodish HF, Carr BI. Growth inhibition by transforming growth factor β (TGF-β) type I is restored in TGF-β-resistant hepatoma cells after expression of TGF-β receptor type II cDNA. Proc Natl Acad Sci USA. 1993;90:5359–63.
24. Hu C, Liu D, Zhang Y, Lou G, Huang G, Chen B, et al LXRα-mediated downregulation of FOXM1 suppresses the proliferation of hepatocellular carcinoma cells. Oncogene. 2014;33:2888–97.
25. Vedin LL, Lewandowski SA, Parini P, Gustafsson J-A, Steffensen KR. The oxysterol receptor LXR inhibits proliferation of human breast cancer cells. Carcinogenesis. 2009;30:575–9.
26. Kim KH, Lee GY, Kim JI, Ham M, Won Lee J, Kim JB. Inhibitory effect of LXR activation on cell proliferation and cell cycle progression through lipogenic activity. J Lipid Res. 2010;51:3425–33.
27. Candelaria NR, Addanki S, Zheng J, Nguyen-Vu T, Karaboga H, Dey P, et al Antiproliferative effects and mechanisms of liver X receptor ligands in pancreatic ductal adenocarcinoma cells. PLoS ONE. 2014;9:e106289.
28. Franco DL, Mainez J, Vega S, Sancho P, Murillo MM, de Frutos CA, et al Snail1 suppresses TGF-β-induced apoptosis and is sufficient to trigger EMT in hepatocytes. J Cell Sci. 2010;123:3467–77.
29. Vega S, Morales AV, Ocana OH, Valdes F, Fabregat I, Nieto MA. Snail blocks the cell cycle and confers resistance to cell death. Genes Dev. 2004;18:1131–43.
30. Caja L, Sancho P, Bertran E, Iglesias-Serret D, Gil J, Fabregat I. Overactivation of the MEK/ERK pathway in liver tumor cells confers resistance to TGF-β-induced cell death through impairing up-regulation of the NADPH oxidase NOX4. Cancer Res. 2009;69:7595–602.
31. Carmona-Cuenca I, Roncero C, Sancho P, Caja L, Fausto N, Fernandez M, *et al* Upregulation of the NADPH oxidase NOX4 by TGF-β in hepatocytes is required for its pro-apoptotic activity. J Hepatol. 2008;49:965–76.
32. Reichl P, Dengler M, van Zijl F, Huber H, Fuhrlinger G, Reichel C, et al Axl activates autocrine transforming growth factor-β signaling in hepatocellular carcinoma. Hepatology. 2015;61:930–41.
33. Thuault S, Tan E-J, Peinado H, Cano A, Heldin C-H, Moustakas A. HMGA2 and Smads co-regulate SNAIL1 expression during induction of epithelial-to-mesenchymal transition. J Biol Chem. 2008;283:33437–46.